ISSN 1028-334X, Doklady Earth Sciences, 2006, Vol. 411, No. 8, pp. 1284–1288. © Pleiades Publishing, Inc., 2006.
Original Russian Text © O.M. Belotserkovskii, I.V. Mingalev, V.S. Mingalev, O.V. Mingalev, A.M. Oparin, 2006, published in Doklady Akademii Nauk, 2006, Vol. 410, No. 6, pp. 816–820.

GEOPHYSICS

Mechanism of the Appearance of a Large-Scale Vortex in the Troposphere above a Nonuniformly Heated Surface

Academician of the RAS O. M. Belotserkovskii[a], I. V. Mingalev[b], V. S. Mingalev[b], O. V. Mingalev[b], and A. M. Oparin[a]

Received April 26, 2006

DOI: 10.1134/S1028334X06080277

.This paper is dedicated to a numerical modeling study of the formation mechanisms of a large-scale vortex over a warm water band on the ocean surface. For this purpose, we developed a 3D model of the atmospheric circulation in a domain, which is a part of spherical layer over a limited region of the Earth's surface (altitude 15 km, longitude and latitude 12°). This model takes into account heating/cooling of the air due to absorption/emission of infrared radiation, as well as due to phase transitions of water vapor to microdrops of water and ice particles, which play an important role. Air transport in the troposphere over a warm region at the ocean surface was numerically simulated using the developed model under different physical conditions. The modeling results allowed us to distinguish the mechanism of cyclone formation over the ocean.

BRIEF DESCRIPTION OF THE MODEL

It is known that tropical cyclones are the strongest large-scale vortex motions in the troposphere. They form over the ocean in the 30° S–30° N equatorial region over patches of warm water with a temperature not less than 26°C and with a temperature difference between the warm patch and the surrounding water of not less than 3°C [1]. During cyclone formation, the air motion in the cyclone is significantly three-dimensional.

In this model, the atmospheric gas is considered a mixture of air and water vapor, in which two types of aerosols (water microdrops and ice microparticles) can exist. We consider that water microdrops and ice microparticles are spheres (radius equal to 0.1 mm and 0.03 mm, respectively), which move (relative to the mixture of air and water vapor) with precipitation velocity in an external force field equal to $\mathbf{v}_w^{prec}$ and $\mathbf{v}_i^{prec}$ determined from the Stokes relation with Cunningham's correction. The chosen sizes of aerosol particles correspond to real mean sizes of particles in the clouds. We assume that the temperature of the mixture is the same as that of the aerosol particles and denote it as T. We also assume that the aerosol of water drops can exist only in the condition of saturated water vapor and $T \geq T_0 = 273.15$K, while the aerosol of ice particles can exist only in the condition of water vapor saturation and $T \leq T_0$. At $T = T_0$, the temperature of the medium cannot increase until all ice particles melt and it cannot decrease until all water drops freeze. The dependence of the density of the saturated vapor ρ_v^{max} on temperature is given by the equation

$$\rho_v^{max}(T) = \left(\frac{T}{T_0}\right)^a \exp\left(\frac{b(T-T_0)}{TT_0}\right)\frac{p_0^{max}}{R_v T}, \qquad (1)$$

where p_0^{max} is the pressure of the saturated vapor at $T = T_0$, and parameters a and b are determined from the following formulas:

at $T \geq T_0$,

$$a = \left(\frac{3}{2} - \frac{C_w}{R_v}\right), \quad b = \frac{q_{ev}^0 - T_0(3R_v/2 - C_w)}{R_v},$$

at $T < T_0$,

$$a = \left(\frac{3}{2} - \frac{C_i}{R_v}\right), \quad b = \frac{q_{ev}^0 + q_{mel} - T_0(3R_v/2 - C_i)}{R_v},$$

where R_v is the gas constant of water vapor; q_{ev}^0 is the specific heat of water evaporation at $T = T_0$; q_{mel} is the specific heat of ice melting at $T = T_0$; and C_w and C_i are specific heat capacities of water and ice, respectively, which are assumed constant. The dependence given by Eq. (1) agrees well with the exponent dependence.

[a] *Institute of Automated Design, Russian Academy of Sciences, Vtoraya Brestskaya ul. 19/18, Moscow, 123056 Russia; e-mail: a.oparin@icad.org.ru*

[b] *Polar Geophysical Institute, Kola Scientific Center, Russian Academy of Sciences, ul. Fersmana 14, Apatity, Murmansk oblast, 184200 Russia*

In the model, the following variables are calculated at each note of the grid: temperature T; densities of air and water vapor ρ_a and ρ_v, respectively; hydrodynamic velocity of the mixture (a 3D vector) $\mathbf{v}$; and the total mass of water drops ρ_w and ice particles ρ_i in a unit volume. The model equations include the equations of continuity for air and for the total water content in all phase states, the equation for 3D velocity of air in a conservative form, and the equation for the total energy in a unit volume of the medium W:

$$\frac{\partial \rho_a}{\partial t} + \mathrm{div}(\rho_a \mathbf{v}) = 0, \quad (2)$$

$$\frac{\partial(\rho_v + \rho_w + \rho_i)}{\partial t} + \mathrm{div}(\rho_v \mathbf{v} + \rho_w(\mathbf{v} + \mathbf{v}_w^{\mathrm{prec}}) + \rho_i(\mathbf{v} + \mathbf{v}_i^{\mathrm{prec}})) = 0, \quad (3)$$

$$\frac{\partial(\rho_{\mathrm{mix}} \mathbf{v})}{\partial t} + \mathrm{div}(\rho_{\mathrm{mix}} \mathbf{v} \otimes \mathbf{v}) = (-\nabla p + \mathrm{div}\hat{\mathcal{T}}) + (\rho_{\mathrm{mix}} + \rho_w + \rho_i)\mathbf{F}, \quad (4)$$

$$\frac{\partial W}{\partial t} + \mathrm{div}(W_{\mathrm{mix}} \mathbf{v} + W_w(\mathbf{v} + \mathbf{v}_w^{\mathrm{prec}}) + W_i(\mathbf{v} + \mathbf{v}_i^{\mathrm{prec}})) = (\rho_{\mathrm{mix}} \mathbf{v} + \rho_w(\mathbf{v} + \mathbf{v}_w^{\mathrm{prec}}) + \rho_i(\mathbf{v} + \mathbf{v}_i^{\mathrm{prec}})\mathbf{F}) + \mathrm{div}(\hat{\mathcal{T}} \cdot \mathbf{v} - p\mathbf{v} - \mathbf{j}) + Q, \quad (5)$$

where $\rho_{\mathrm{mix}} = \rho_a + \rho_v$, $p = (\rho_a R_a + \rho_v R_v)T$ is the pressure in the mixture; R_a is the gas constant of air; $\hat{\mathcal{T}}$ is the tensor of viscous stresses; and $\mathbf{F}$ is the acceleration of external forces, which consists of the accelerations due to gravity, the Coriolis force, and centrifugal force. In our model, we assume that the Earth's surface is spherical. Therefore, we do not take into account the meridional component of the centrifugal force, which in reality is compensated by the Earth's nonspherical form. Acceleration $\mathbf{F}$ is specified by the relation

$$\mathbf{F} = -\mathbf{r}\left(\frac{g_0 r_e^2}{r^3} - \Omega^2 + \frac{(\boldsymbol{\Omega}, \mathbf{r})^2}{r^2}\right) + 2[\mathbf{v} \times \Omega],$$

where g_0 is acceleration due to gravity at the poles at the earth's surface; $\mathbf{r}$ is the radius vector from the Earth's center to a given point; r is the length of the radius vector; r_e is the Earth's radius; and $\boldsymbol{\Omega}$ is the vector of the angular velocity of the Earth's rotation. The tensor of viscous stresses $\hat{\mathcal{T}}$ is specified with account for turbulent exchange as a deviator of symmetric tensor $\hat{D}$ using the following relations:

$$\hat{\mathcal{T}} = \hat{D} - \frac{1}{3}\hat{I}\mathrm{Tr}(\hat{D}), \quad \hat{D} = \hat{\eta}(\nabla \mathbf{v}) + (\nabla \mathbf{v})^T \hat{\eta},$$

where $\hat{I}$ is the unit tensor; $\mathrm{Tr}(\hat{D})$ is the trace of tensor $\hat{D}$; $\nabla \mathbf{v}$ is the tensor of the hydrodynamic velocity gradient; $\hat{\eta}$ is the symmetric tensor of coefficients of viscosity, which is diagonal in the geographical coordinate system; and its diagonal components are the sum of the usual dynamic coefficient of molecular viscosity of air and the coefficients of turbulent exchange in the direction of local unit vectors of the geographical coordinate system. The coefficients of turbulent exchange depend on the grid mesh in the direction of the given unit vectors. They are specified using the Richardson formula [2] similarly to the model of the general circulation of the Earth's atmosphere [3]. In addition, the following notations are used in Eq. (5)

$$W = W_{\mathrm{mix}} + W_w + W_i, \quad W_i = \rho_i\left(\frac{(\mathbf{v} + \mathbf{v}_i^{\mathrm{prec}})^2}{2} + C_i T\right),$$

$$W_w = \rho_w\left(\frac{(\mathbf{v} + \mathbf{v}_w^{\mathrm{prec}})^2}{2} + C_w(T - T_0) + q_{\mathrm{mel}} + C_i T_0\right),$$

$$W_{\mathrm{mix}} = \frac{1}{2}\rho_{\mathrm{mix}} \mathbf{v}^2 + \frac{3}{2}\rho_a R_a T + \rho_v\left(\frac{3}{2}R_v(T - T_0) + q_{ev}^0 + q_{\mathrm{mel}} + C_i T_0\right),$$

$\mathbf{j} = -\hat{\lambda}\nabla T$ is the vector of heat flux; $\hat{\lambda}$ is the symmetric tensor of thermal conductivity coefficients, which is diagonal in the geographical coordinate system; the diagonal components are the sum of the usual coefficient of molecular thermal conductivity of air and the coefficients of turbulent exchange in the direction of local unit vectors in the geographical coordinate system; and Q is the rate of release/absorption of energy in a unit volume due to absorption/emission of infrared radiation. A block for calculating infrared radiation transport was included in the model to determine this energy. It is a one-sheet one-dimensional block (integral over all regions of the infrared spectrum range). The coefficients of absorption/emission for air and water vapor depend on altitude. They are defined in the following way: if we use vertical distributions of the temperature/density of air and water vapor (typical of the summertime for the latitude, which encloses the center of the calculation region), the developed block would yield a radiation field coinciding with the results of reference calculations [4], which take into account a large number of spectral intervals in the infrared spectral range.

Temperature T and densities ρ_v, ρ_w, and ρ_i are determined by the values of ρ_a, the sum total $(\rho_v + \rho_w + \rho_i)$, and the volume density of internal energy of the medium

$$E = W - \frac{1}{2}(\rho_{\mathrm{mix}} \mathbf{v}^2 + \rho_w(\mathbf{v} + \mathbf{v}_w^{\mathrm{prec}})^2 + \rho_i(\mathbf{v} + \mathbf{v}_i^{\mathrm{prec}})^2)$$

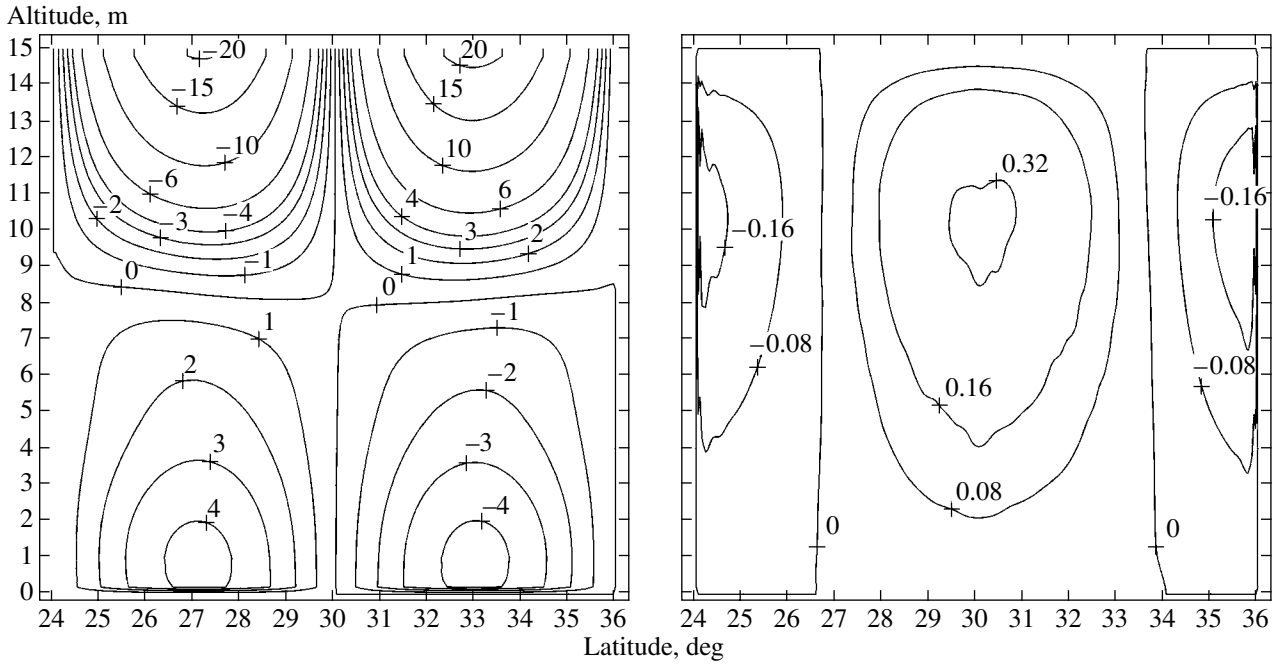

Fig. 1. Distribution of meridional (left) and vertical (right) components of wind velocity (m/s) over a vertical section along the meridian that passes across the patch center 10 h after the beginning of calculations. The northward and upward directions are considered positive.

in four conditions: $\rho_v \le \rho_v^{max}(T)$; $\rho_v = \rho_v^{max}(T)$ at $\rho_w + \rho_i > 0$; $\rho_w = 0$ at $T < T_0$; and $\rho_i = 0$ at $T > T_0$.

The following conditions are specified at the lower boundary of the model region: $\mathbf{v} = 0$; $\rho_v = \rho_v^{max}(T)$, $\rho_w = \rho_i = 0$, and the heat flux is specified proportional to the difference between the air and water temperatures at the surface together with the flux of upward thermal radiation proportional to the fourth power of the temperature at the surface. At the upper boundary of the model region, we specified the slip condition for horizontal velocity components **v** and the zero flow condition for its vertical component, as well as the zero derivative of the vertical component of **j** with respect to altitude and the flux of downward thermal radiation. At the lateral surface of the model region, the derivative of temperature along the normal to this surface and velocity **v** were assumed to be zero.

The initial temperature, air density, and vapor density in the model region were specified as horizontally uniform. The dependence of the initial temperature and air density on altitude was determined from the NRLMSISE-00 empirical model [5] for the center of the calculation region. We considered various versions of the dependence of the vapor density on altitude at the initial moment of time. The initial velocity **v** and initial ρ_w were assumed zero in the entire calculation region.

The calculation grid was taken to be uniform with a step along latitude and longitude equal to 0.04° and with a step along altitude equal to 200 m ($300 \times 300 \times 75$ nodes). System (2)–(5) together with the closing equations is more complicated than the Navier–Stokes system commonly used in numerical simulation [6]. Numerical solution of system (2)–(5) was performed using the implicit iteration (two-layer) finite-difference scheme.

RESULTS

An elongated band was specified in the center of the lower boundary of the modeling region, in the middle of which the temperature was greater by 10 K than beyond this band. The length of the warmest part of the band from south to north was approximately 200 km and the total width of the band in this direction was approximately 400 km. The evolution of parameters in the model region was calculated for several tens of hours at different lengths of the band (400 to 1000 km, from west to east) and at different degrees of air saturation with water vapor at the initial moment, when the air was assumed at rest. An increase in the content of water vapor amplifies significantly the rate of heating/cooling of the atmospheric gas due to absorption/emission of infrared radiation. It was found that if the rate of heating/cooling at altitudes of 0–1 km over the patch differs sufficiently from this rate at a distance from the patch (more than by 8 K/h), then a 3D current is formed within a few hours. In this current, the meridional component of the wind velocity is directed southward (north of the band) and northward (south of the band) in the lower troposphere. In the upper troposphere, this component is directed from the center of the band. The vertical wind component is directed

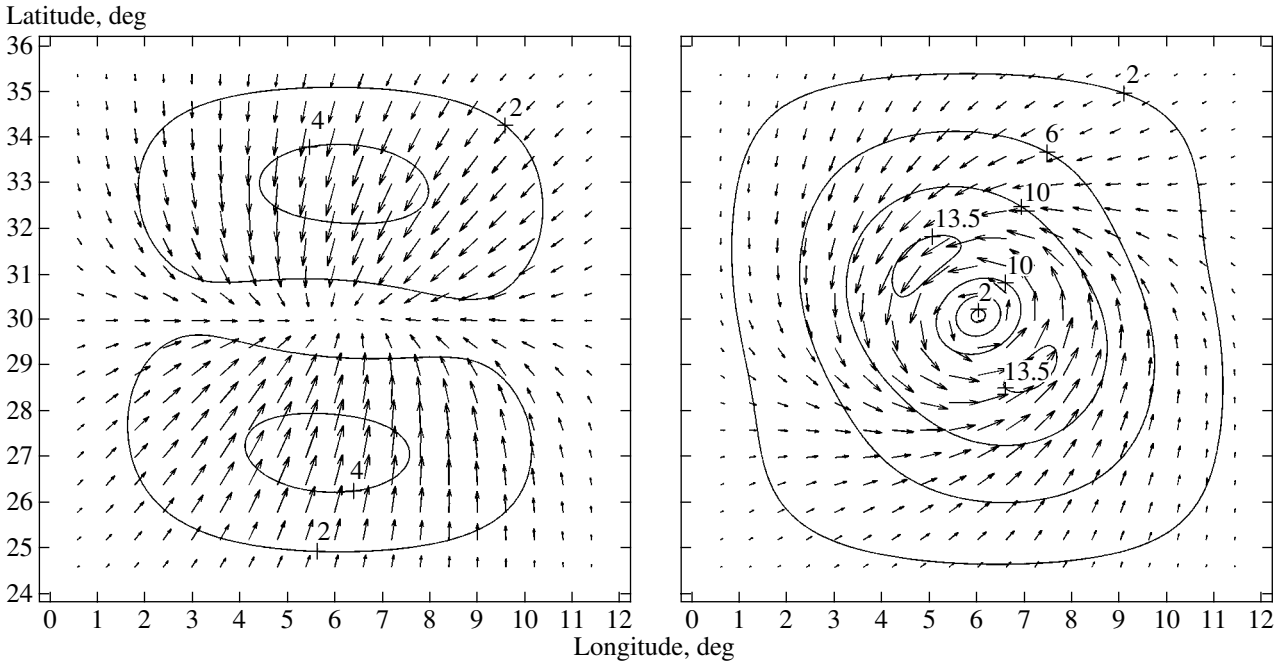

Fig. 2. Distribution of the horizontal component of the wind velocity (m/s) at an altitude of 600 m 10 h (left) and 40 h (right) after the beginning of calculations. The arrows show the direction, and their length and level lines denote the absolute value.

upward above the band and downward beyond the band. The current develops most rapidly if the air is saturated with wind vapor at the initial moment. Figures 1 and 2 show the modeling results for the case when the length of the W–E band was approximately 1000 km. Figure 1 depicts the distribution of meridional (left) and vertical (right) components of the wind velocity (m/s) 10 h after the beginning of the calculation on a vertical meridional section across the center of the band. It is seen that the vertical velocity component exceeds 0.3 m/s above the center of the band at altitudes of 9–11 km. It is also seen that at altitudes of 0–8 km, the meridional component of the velocity is directed to the center of the band and exceeds 4 m/s at altitudes of 0–2 km. At altitudes of 9–15 km, this component is directed from the center of the band and exceeds 20 m/s at an altitude of 15 km. In the course of time, this current varies smoothly. Due to the Coriolis force, a rotating component appears at an altitude of 6 km in the distribution of the horizontal component of velocity with respect to the center of the patch. Figure 2 shows the distribution of the horizontal component of wind velocity (m/s) at an altitude of 600 m 10 h (left) and 40 h (right) after the beginning of calculations. The appearance of the rotating component of the velocity field with respect to the center of the band is seen in the right part of Fig. 2.

The calculations also showed that if, at the initial moment, the relative air humidity is less than 60%, the velocity in the appearing current is several times slower than those in Figs. 1 and 2. In addition, if the length-to-width ratio for the warmest part of the band is smaller than 1: 3, no notable rotation around the center of the patch appears within 40 h.

CONCLUSIONS

Thus, our results of numerical simulation of the initial phase of cyclone formation point to the following fact: the formation of a cyclone requires the presence of water vapor-saturated warm air masses in the troposphere above a sufficiently distal (relative to equator) west-to-east-oriented warm water band surrounded by colder waters. The horizontal size of this region occupied with air masses should be not less than a few hundred kilometers. The mechanism of cyclone formation in air masses at rest is as follows. Due to the loss of energy caused by the thermal radiation, the air mass cools in the lower troposphere beyond the warm band and its pressure decreases, resulting in the descent of air from the overlying layers. However, the air above the band warms up due to the absorption of thermal radiation from the surface, resulting in the formation of an ascending current. These processes generate a horizontal current with the following characteristics: in the lower troposphere, the meridional component of the wind velocity is directed southward (north of the band) and northward (south of the band). In the upper troposphere, this component is directed from the center of the band. If the horizontal size of this current and wind velocity are sufficiently great, then the Coriolis force in the lower troposphere turns the current to the west (north of the band) and east (south of the band). This leads to curling of the current and formation of a cyclonic vortex with a vertical axis located near the center of the warm water band. In a time period shorter than two days, the transversal velocity can increase from zero to more than 13 m/s at a distance of ~180 km from the vortex axis.

ACKNOWLEDGMENTS

This work was supported by the Presidium of the Russian Academy of Sciences (Multidisciplinary Program no. 14 "Fundamental Problems of Informatics and Information Technologies").

REFERENCES

1. L. T. Matveev, *Theory of General Circulation of the Atmosphere and Earth's Climate* (Gidrometeoizdat, Leningrad, 1991) [in Russian].
2. A. M. Oboukhov, *Turbulence and Atmosphere Dynamics* (Gidrometeoizdat, Leningrad, 1988) [in Russian].
3. I. V. Mingalev and V. S. Mingalev, Mat. Modelirovaniye **17** (5), 24 (2005).
4. A. N. Trotsenko and B. A. Fomin, Izv. Physics Atmosph. and Ocean, **25** (1), 106 (1989).
5. J. M. Picone, A. E. Hedin, D. P. Drob, and A. C. Aikin, J. Geophys. Res. **107** (A12), 1468 (2002).
6. O. M. Belotserkovskii, V. A. Andrushchenko, and Yu. D. Shevelev, *Dynamics of Spatial Vortex Currents in Nonuniform Atmosphere: A Computational Experiment* (Yanus-K, Moscow, 2000) [in Russian].